Supplementary Information

1. We have checked out the results by using different functional. We show respectively the band structures of $MnPSe_3$ from LDA, GGA-PBE and HSE06 functional in Fig. S1. We can see that the curves of band structures are similar especially for the bands near the band gap, although the band gap is different under the different functional. It is well known that the band gap under HSE06 is larger than these under GGA-PBE and LDA. Because our interests mainly focus on the valley and spin character near the band gap in this paper, our results and conclusion are robust for the different functional.
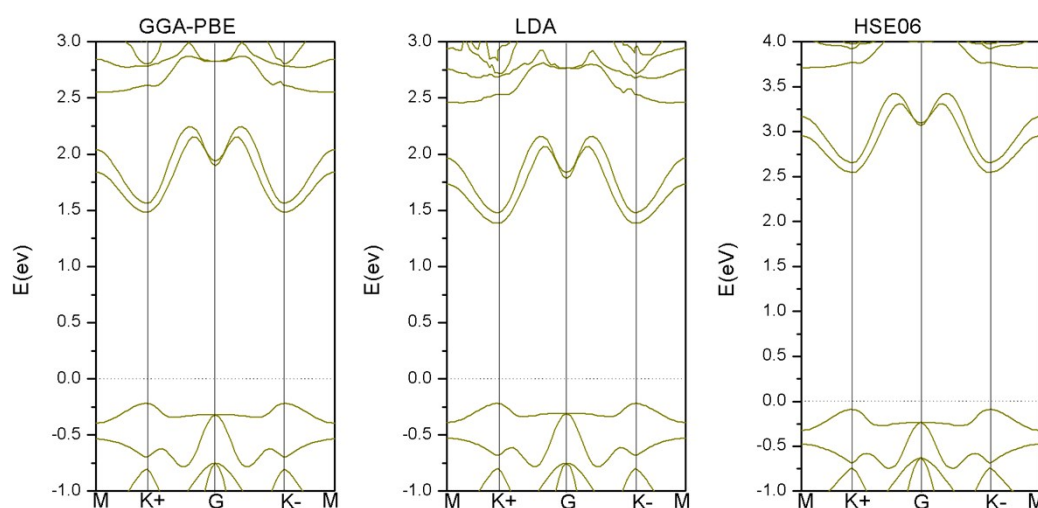

Fig.S1. The band structures of $MnPSe_3$ monolayer under LDA, GGA-PBE and HSE06 functional.

2. We have calculated the band structures of monolayer $MnPS_3$, $MnPSe_3$ and $MnPTe_3$ by the first-principles calculations. The band structures are shown in Fig.S2.
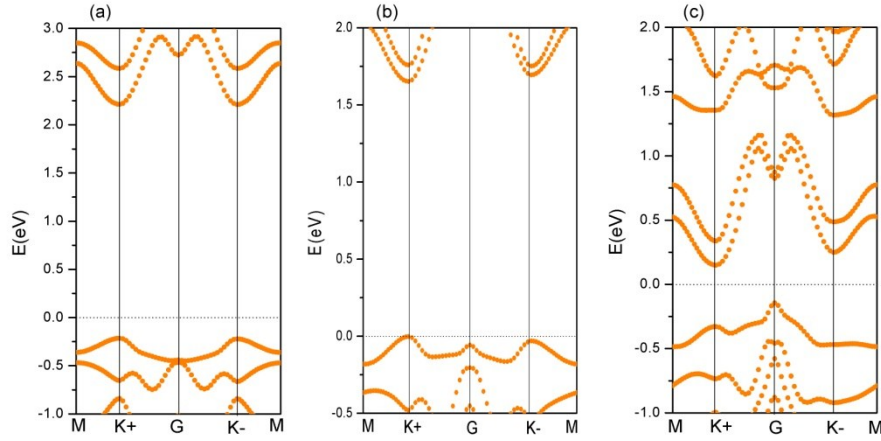
Fig.S2. The band structures of MnPS$_3$(a), MnPSe$_3$(b) and MnPTe$_3$(c) monolayer.

3. We have also calculated V, Cr, Fe, Co, Ni, and Cu doped monolayer MnPSe$_3$. The band structures are showed in Fig.S3 for Mn:X=7:1 and in Fig.S4 for Mn:X=1:1 (X= V, Cr, Fe, Co, Ni, Cu and Zn), respectively. We can see that for the low concentration doping (Mn:X=7:1), the valley character can be preserved for V, Fe, Co, Ni and Zn doped MnPSe$_3$. But the spin splitting is small (<50meV) for V, Fe, Co and Ni doped cases. On the other hand, for the high concentration doping (Mn:X=1:1), the valley character can be preserved for Fe and Zn doped MnPSe$_3$. But the spin splitting is still small (about 50meV) for Fe doped case. So, the most suitable doping element for the realization of larger valley and spin splitting in monolayer MnPSe$_3$ is Zn.
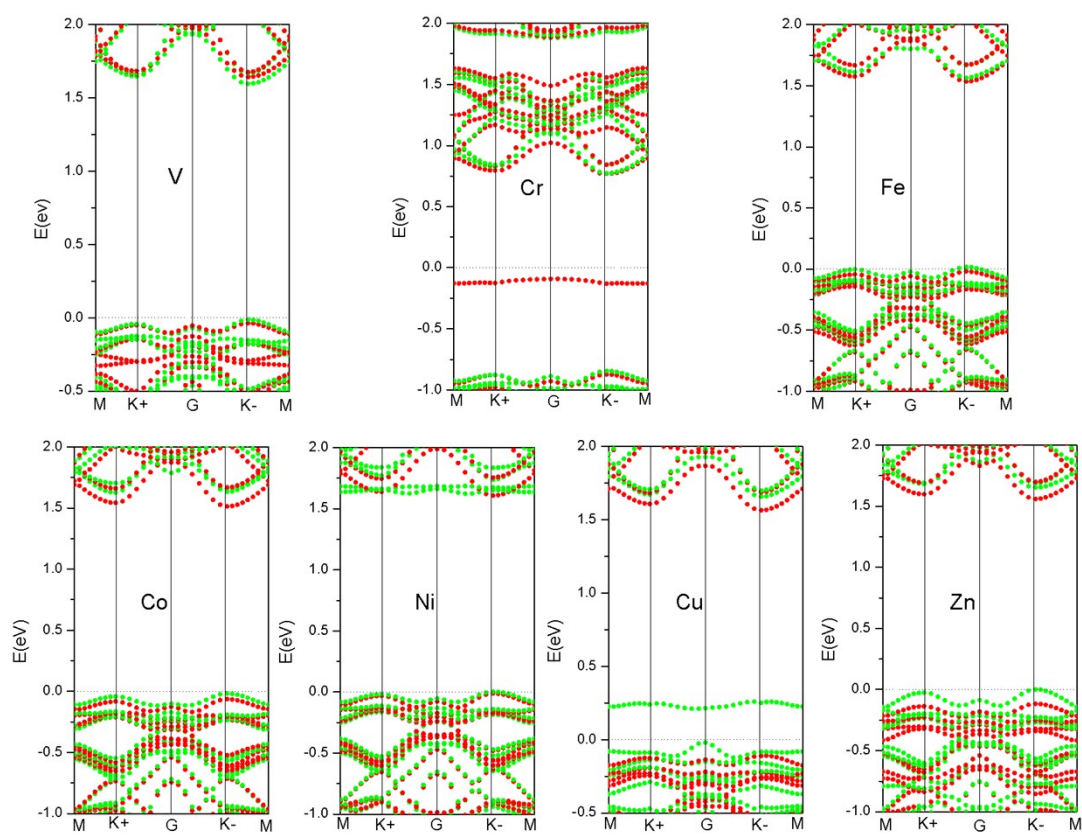
Fig.S3. The band structures of Mn:X=7:1 (X=V,Cr,Fe,Co,Ni,Cu and Zn) doped monolayer MnPSe₃.
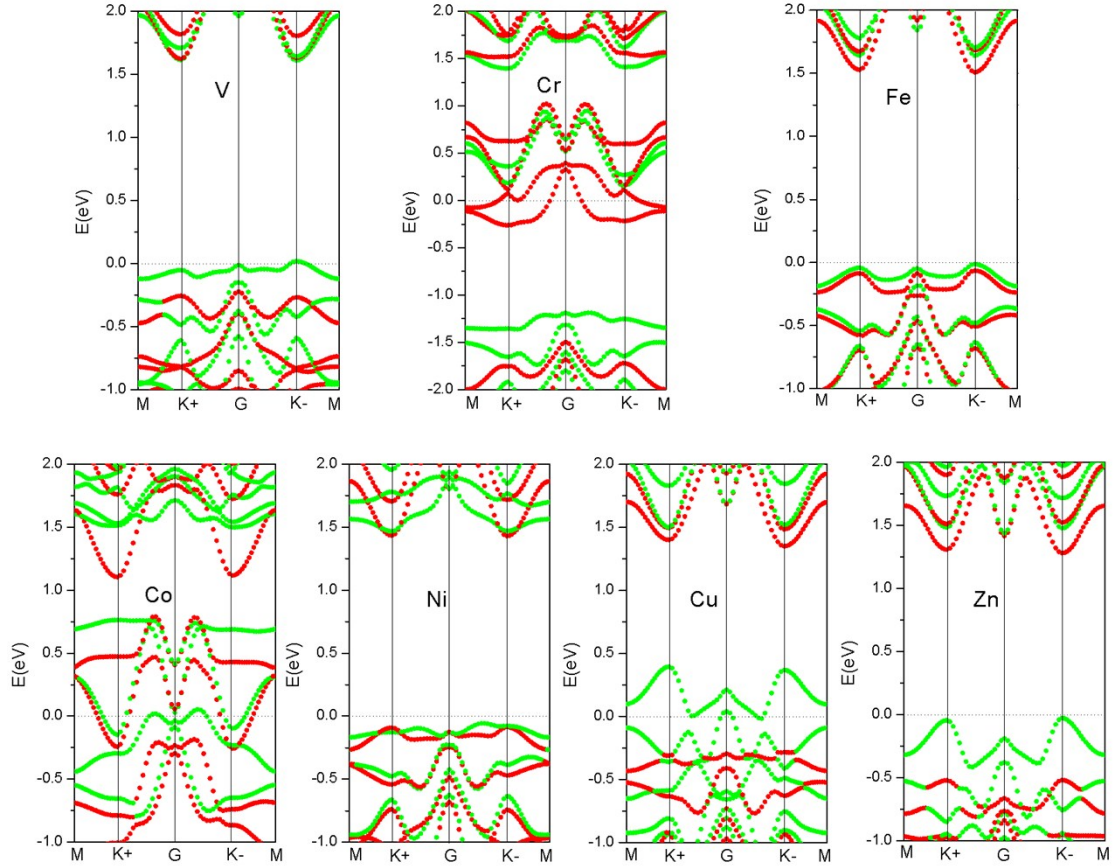
Fig.S4. The band structures of Mn:X=1:1 (X=V,Cr,Fe,Co,Ni,Cu and Zn) doped monolayer MnPSe$_3$.

4. We have also calculated the total energy of Zn-doped MnPSe$_3$ with different positions including Zn-Zn dimer cases, as shown as in Fig. S5. We find that the closer the Zn atom is, the lower the total energy of the system is (see Table.S2). This indicates that the doped Zn atoms will be inclined to occupy Zn-Zn dimer position. For obtaining the uniform magnetization distribution, Zn-Zn dimer needs to be avoided in experiment. This may be kinetically inhibited by the diffusion barrier at a very low temperature. In addition, low concentration doping is also more favorable for preventing the doped Zn atoms from diffusing to form Zn-Zn dimer.
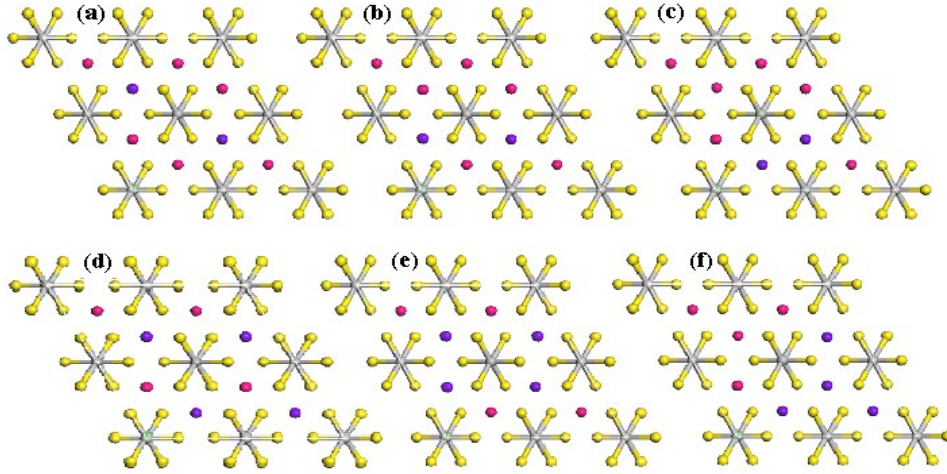
Fig. S5. Different doping positions including Zn-Zn dimer cases. The blue atoms are Zn, red atoms are Mn, gray atoms are P and yellow atoms are Se.

Table.S1 Important energy scales (meV) of HVB, LCB and valley splitting in monolayer $MnPS_3$, $MnPSe_3$ and $MnPTe_3$.

E（meV）	HVB(K_+)	LCB(K_+)	HVB(K_-)	LCB(K_-)	Δvalley(v)	Δvalley(c)
$MnPS_3$	-19.1	2431.4	-25.9	2427	5.8	4.4
$MnPSe_3$	-3.2	1651.8	-41.3	1694.4	28.2	42.6
$MnPTe_3$	-328.9	149.06	-469.36	248.74	104.46	99.68

Table. S2. Total energy of different doping positions.

Mn:Zn=6:2	(a)	(b)	(c)
Total energy	-184.58069124eV	-184.58144397 eV	-184.58231462eV
Mn:Zn=4:4	(d)	(e)	(f)
Total energy	-171.17905288 eV	-171.20260841 eV	-172.77247775 eV